On the AGN origin of μG Magnetic Fields in the Intracluster Medium

Hao Xu

Los Alamos National Lab

Collaborators: Hui Li, Shengtai Li (LANL)
David Collins, Michael Norman (UCSD)

Xu et al. 2010, “Evolution and Distribution of Magnetic Fields from AGNs in Galaxy Clusters. I. The Effect of Injection Energy and Redshift” Ap. J. submitted

Xu et al. 2009, “Turbulence and Dynamo in Galaxy Cluster Medium: Implications on the Origin of Cluster Magnetic Fields”, Ap. J. Lett., 698, L14

Evidence for Cluster Magnetic Fields: Radio Halos and Relics

over 50 now known ➔ cluster mergers

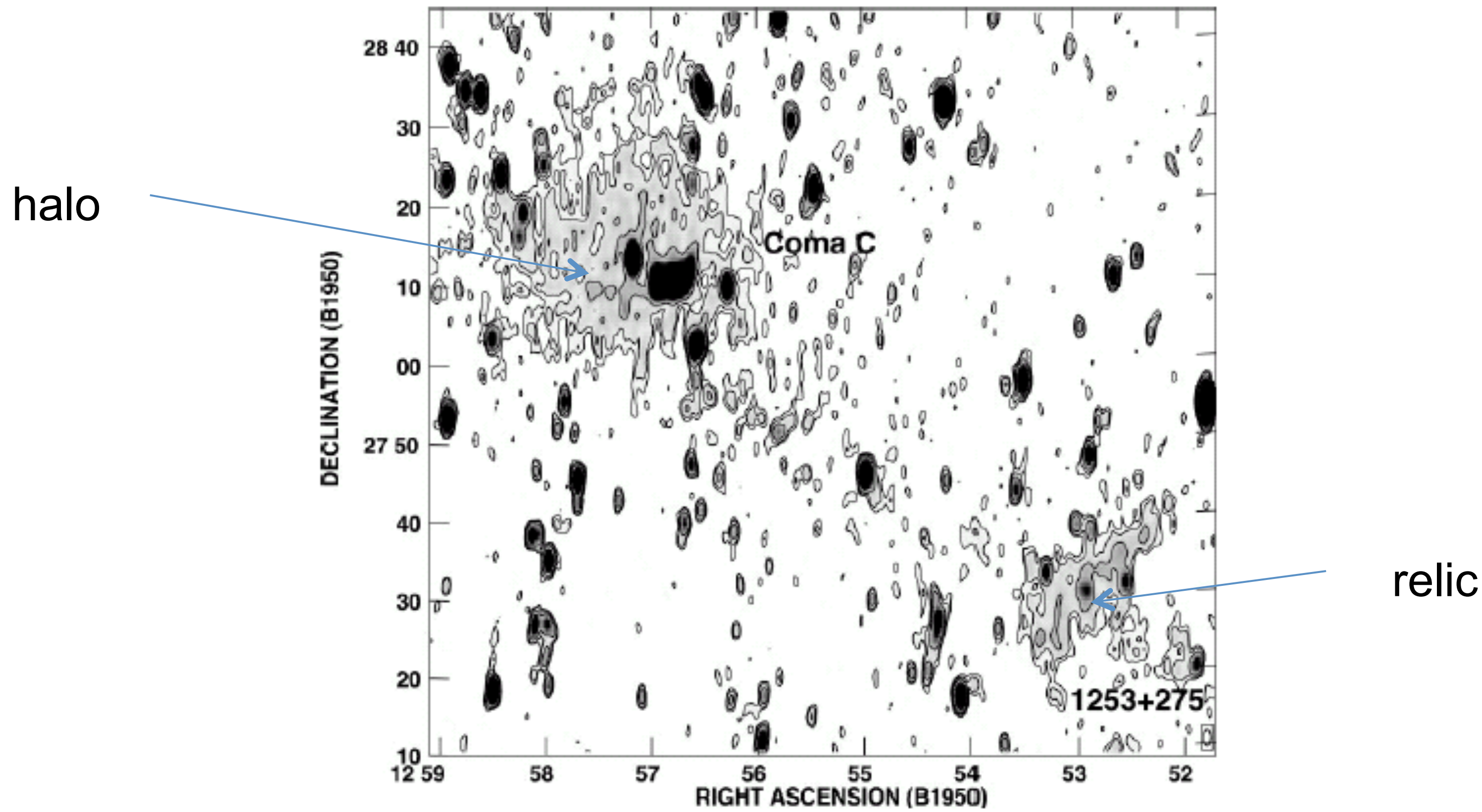

WSRT @ 90 cm

Feretti & Giovannini 1998

Rotation Measure Maps of Cluster Radio Sources

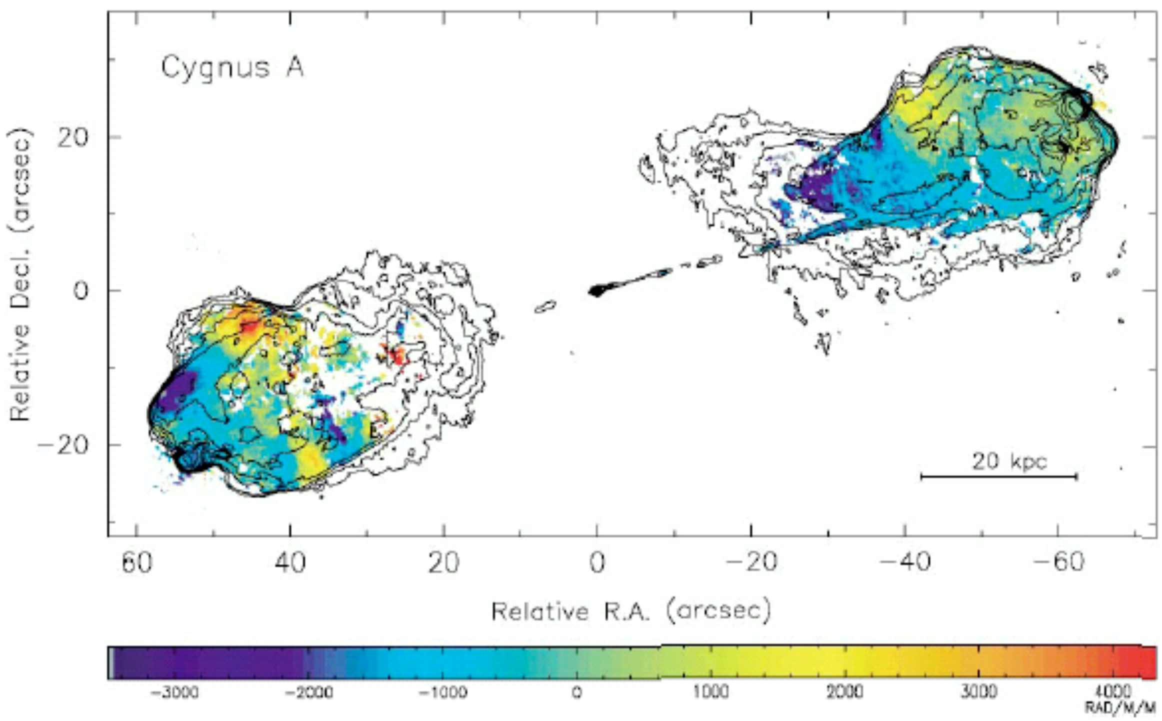

Figure 2 The RM distribution in Cygnus A based on multifrequency, multiconfiguration VLA observations. The resolution is 0.35″ (Dreher, Carilli & Perley 1987). The colorbar indicates the range in RMs from −3400 to +4300 rad m^{-2}. Note the undulations in RM on scales of 10–30 kpc. Contours are overlaid from a 5 GHz total intensity image. The RM was solved for by fitting for the change in polarization angle with frequency on a pixel-by-pixel basis (see Figure 4).

RM versus radius

- Sample of 16 radio halo clusters
- Measured RM due to background and embedded radio sources
- All exhibit magnetic fields out to edge of X-ray emission ~1 Mpc

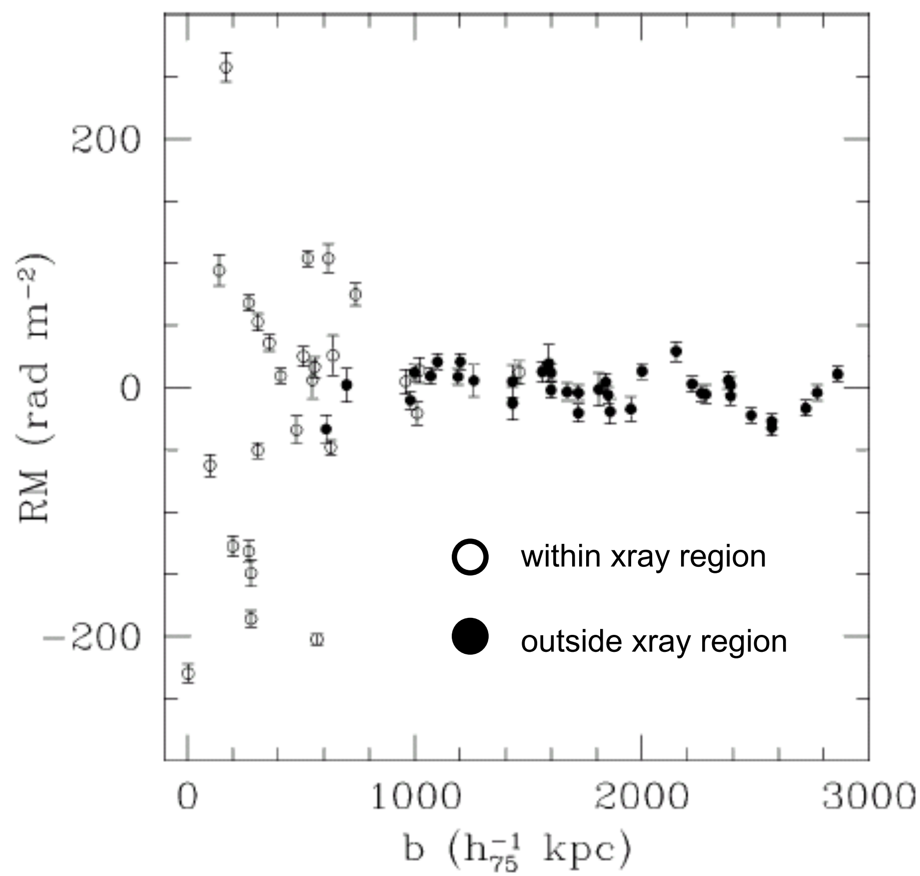

Clarke, Kronberg & Boehringer (2001)

Measuring Cluster Magnetic Fields

- Synchrotron emission
  - Equipartition assumption between B and n_{rel} yields B from radio surface brightness (Burbidge 1959)
- Faraday rotation

$$\boxed{RM = \frac{\chi_{pol}}{\lambda^2} = 812\int\left(\frac{n_e}{cm^{-3}}\right)\left(\frac{\vec{B}}{\mu G}\right)\cdot\left(\frac{d\vec{\ell}}{kpc}\right)\,\mathrm{rad/m^2}}$$

  - B depends on assumed field correlation length
- Inverse Compton X-ray emission
  - If same rel. electrons responsible for radio synchrotron and IC x-rays, then

$$\boxed{\frac{L_{synch}}{L_{IC}} \propto \frac{U_{mag}}{U_{rad}} \Rightarrow B = 1.7(1+z)^2\left(\frac{S_r\nu_r}{S_x\nu_x}\right)^{0.5}\mu G}$$

Summary of Observations

TABLE 1 Cluster magnetic fields

Method	**Strength μG**	**Model parameters**
Synchrotron halos	0.4–1	Minimum energy, $k = \eta = 1$, $\nu_{\rm low} = 10$ MHz, $\nu_{\rm high} = 10$ GHz
Faraday rotation (embedded)	3–40	Cell size = 10 kpc
Faraday rotation (background)	1–10	Cell size = 10 kpc
Inverse Compton	0.2–1	$\alpha = -1$, $\gamma_{\rm radio} \sim 18000$, $\gamma_{\rm xray} \sim 5000$
Cold fronts	1–10	Amplification factor $\sim$3
GZK	$>$0.3	AGN = site of origin for EeV CRs

Carilli & Taylor 2002

Possible Origins for Cluster B-fields

- Magnetized jets and winds from galaxies and AGN
- Ram-pressure stripping of cluster galaxy interstellar fields
- Compression of intergalactic fields
- Biermann battery seed fields generated during structure formation, amplified by cluster turbulence

Our Hypothesis

- A single injection of B-fields by an AGN is sufficient to magnetize the entire cluster to observed levels if
  - injection is early enough
  - major mergers induce cluster-wide turbulence

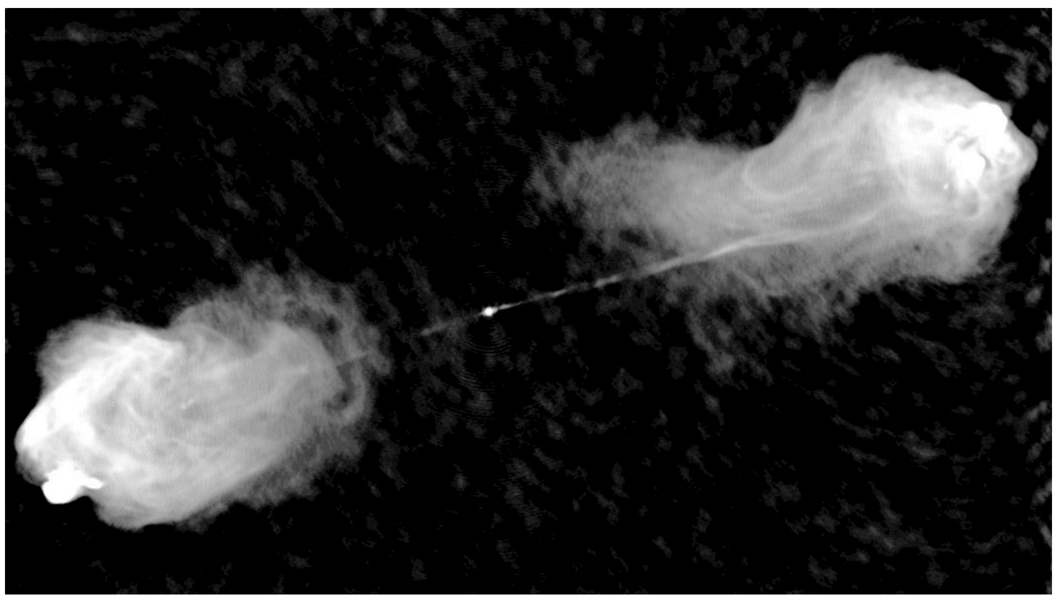

Cluster Assembly

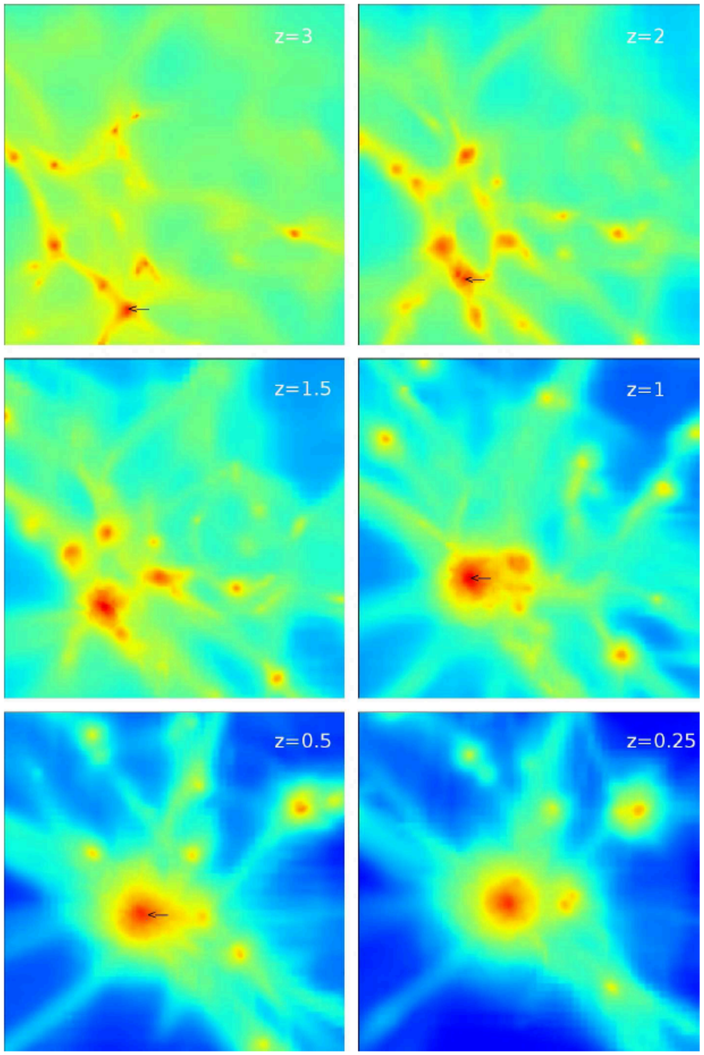

- Cluster mass assembled through mergers of sub-clusters between z=2-1
- Drives strong turbulence

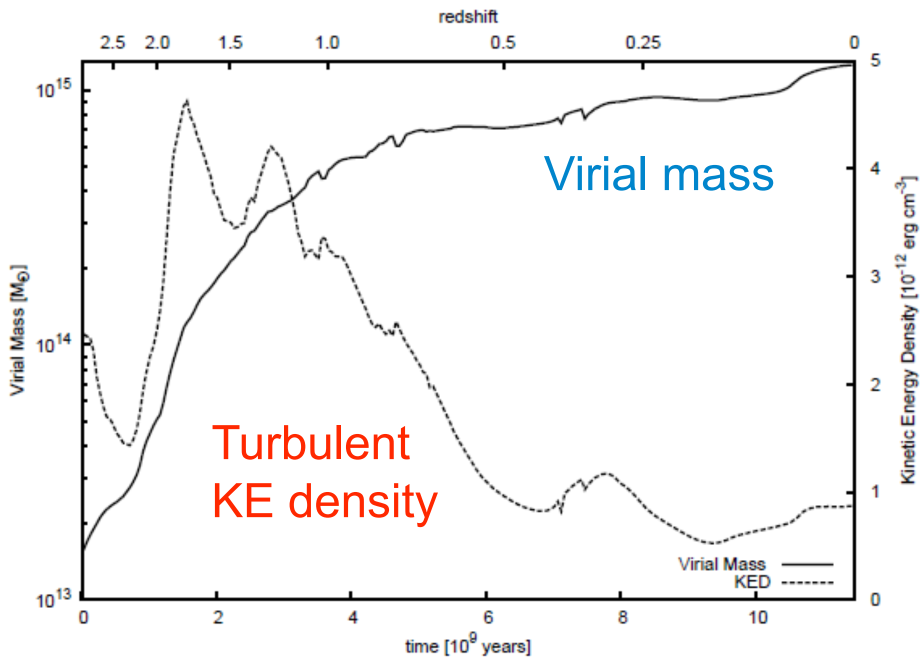

What we did

- Performed cosmological AMR MHD simulation of galaxy cluster formation using newly developed ENZO-MHD code
  - Inject magnetic jet at z=3 for 36 Myr and then evolve ICM to the present epoch
  - See what happens to injected field
  - Maintain uniform 11 kpc resolution throughout cluster-forming region wherever $B>5 \times 10^{-8}$ G
  - ➔effectively a 600^3 uniform grid tracking cluster-forming region within cosmological simulation

Cosmological AMR MHD in ENZO

Collins et al. (2010)

$$\frac{\partial \rho}{\partial t} + \frac{1}{a}\nabla \cdot (\rho \mathbf{v}) = 0 \qquad (1)$$

$$\frac{\partial \rho \mathbf{v}}{\partial t} + \frac{1}{a}\nabla \cdot \left(\rho \mathbf{v}\mathbf{v} + \bar{p} - \frac{\mathbf{B}\mathbf{B}}{a}\right) = -\frac{\dot{a}}{a}\rho \mathbf{v} - \frac{1}{a}\rho \nabla \Phi \qquad (2)$$

$$\frac{\partial E}{\partial t} + \frac{1}{a}\nabla \cdot \left[\mathbf{v}(\bar{p} + E) - \frac{1}{a}\mathbf{B}(\mathbf{B}\cdot \mathbf{v})\right] = -\frac{\dot{a}}{a}\left(\rho v^2 + \frac{2}{\gamma - 1}p + \frac{B^2}{2a}\right) - \frac{\rho}{a}\mathbf{v}\cdot \nabla \Phi \qquad (3)$$

$$\frac{\partial \mathbf{B}}{\partial t} - \frac{1}{a}\nabla \times (\mathbf{v} \times \mathbf{B}) = 0 \qquad (4)$$

with the equation of state

$$E = \frac{1}{2}\rho \mathbf{v}^2 + \frac{p}{\gamma - 1} + \frac{1}{2}\mathbf{B}^2$$

$$\bar{p} = p + \frac{1}{2}B^2.$$

$$\rho_{\mathrm{proper}} = \rho a^3, \qquad (7)$$

$$p_{\mathrm{proper}} = p a^3, \qquad (8)$$

$$\mathbf{v}_{\mathrm{proper}} = \mathbf{v} - \dot{a}\mathbf{x}, \qquad (9)$$

$$\Phi_{\mathrm{proper}} = \Phi - \tfrac{1}{2}a\ddot{a}\mathbf{x}^2, \qquad (10)$$

$$\mathbf{B}_{\mathrm{proper}} = \mathbf{B}a^{-2}. \qquad (11)$$

Numerical methods

+Structured AMR (Berger & Collela)

+TVD MHD patch solver (Li & Li)

+CT field evolution (Gardner & Stone)

+Divergence free reconstruction (Balsara)

+Dual energy formulation (Bryan et al.)

Magnetic Jet Injection

- Li et al. (2006) magnetic tower model

Poloidal flux function

$$\Psi(r,\ z) = r^2 \exp(-r^2 - z^2),$$

Poloidal B-field

$$B_{\mathrm{inj},r} = -\frac{1}{r}\frac{\partial \Psi}{\partial z} = 2zr \exp(-r^2 - z^2),$$

$$B_{\mathrm{inj},z} = \frac{1}{r}\frac{\partial \Psi}{\partial r} = 2(1 - r^2) \exp(-r^2 - z^2).$$

Toroidal B-field

$$B_{\mathrm{inj},\phi} = \frac{\alpha \Psi}{r} = \alpha r \exp(-r^2 - z^2),$$

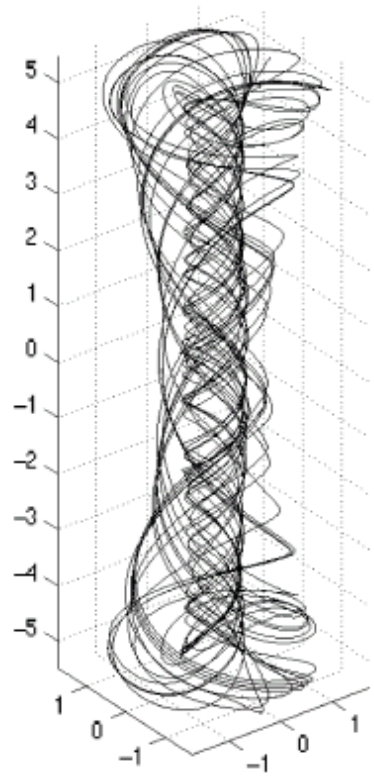

Scaling parameters:

B_0 = source field normalization
L = source region size
α = toroidal/poloidal flux ratio

$$\boxed{E_{mag} \propto \alpha^2 B_0^2 L^3}$$

AGN injection into z=3 protocluster

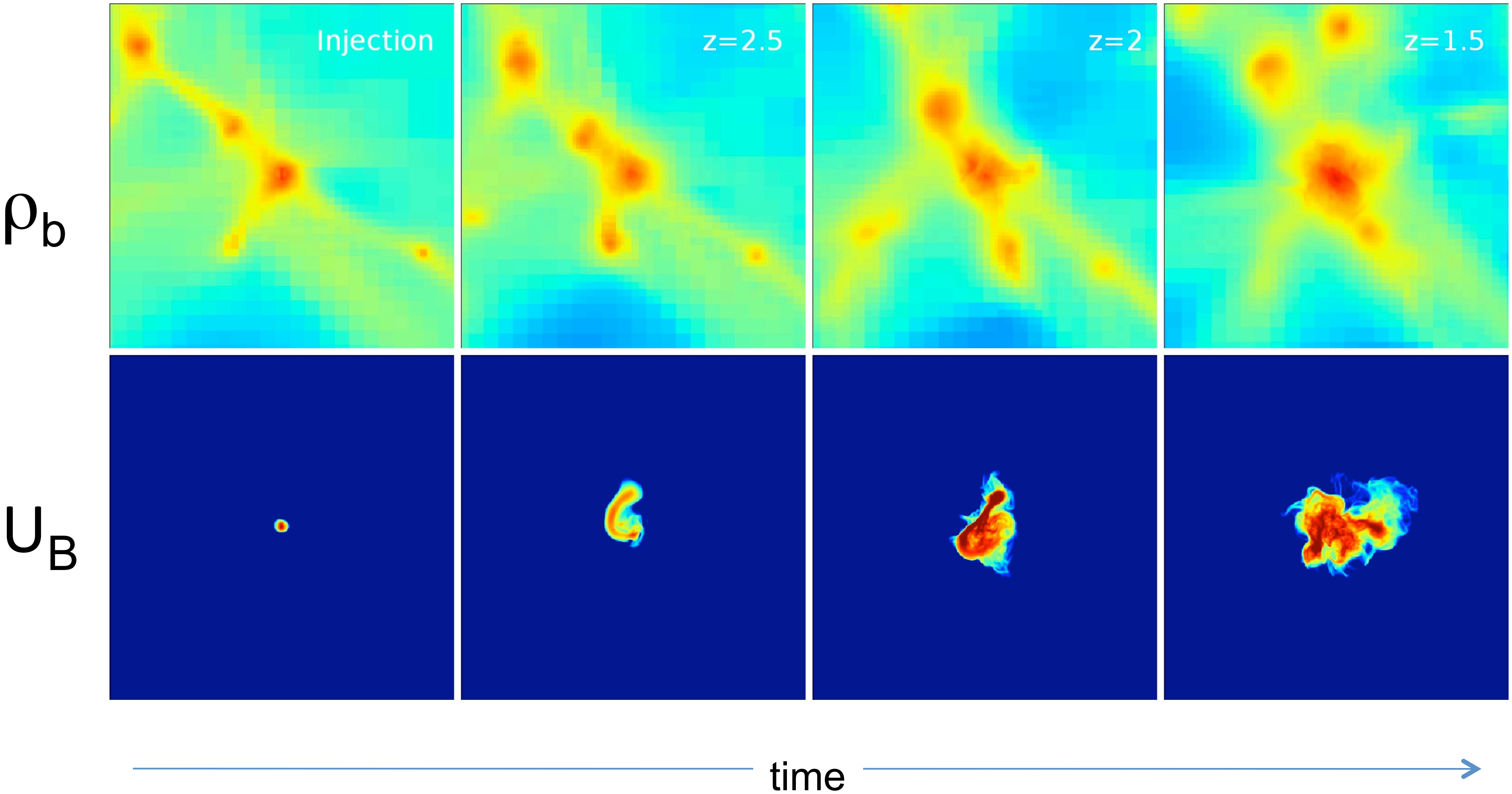

AGN injection into z=3 protocluster

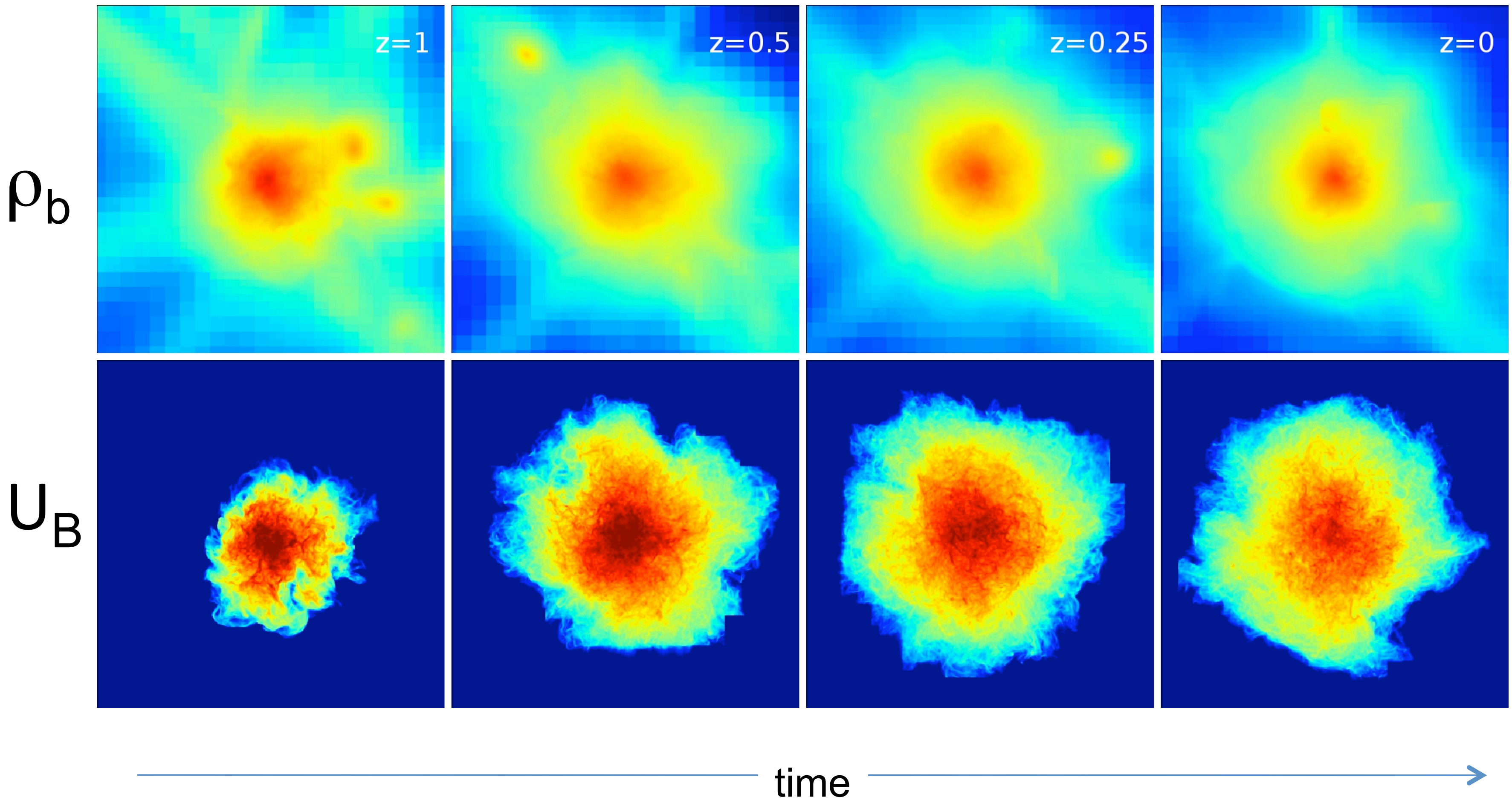

Evolution of Energies

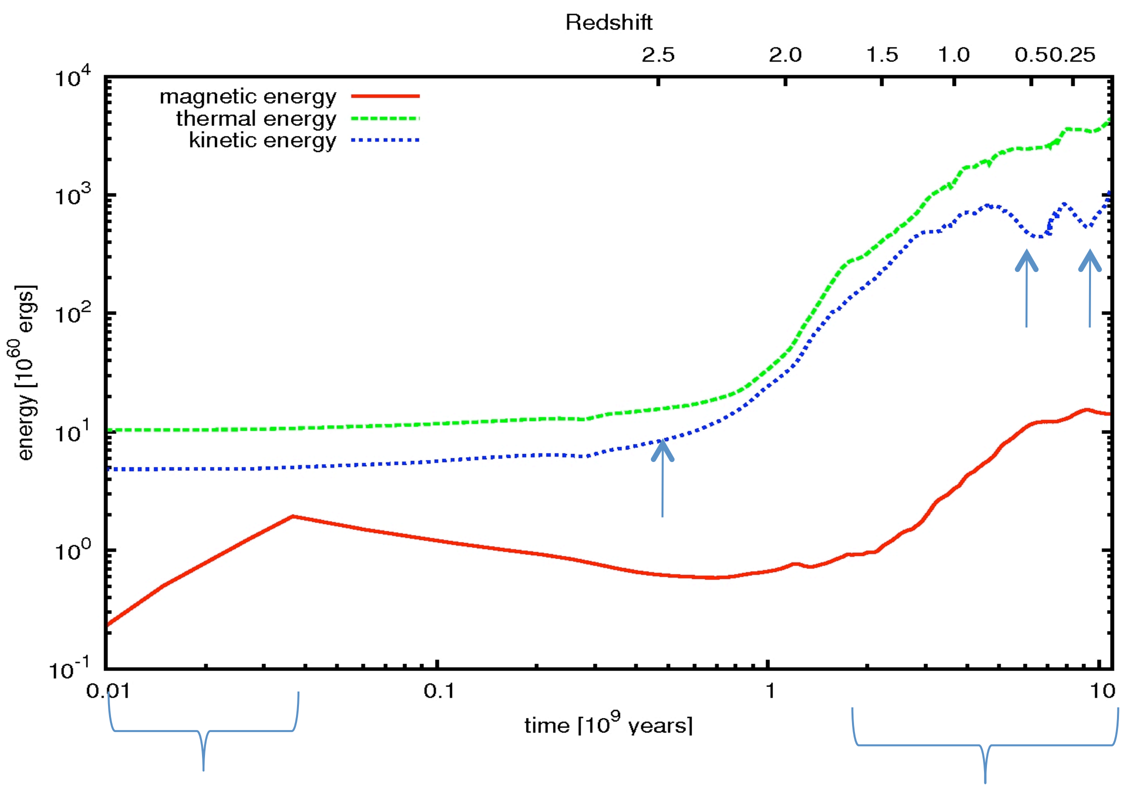

36 Myr injection phase

major merger

turbulent amplification by "small-scale dynamo"

Power spectra in 5.5 Mpc cube

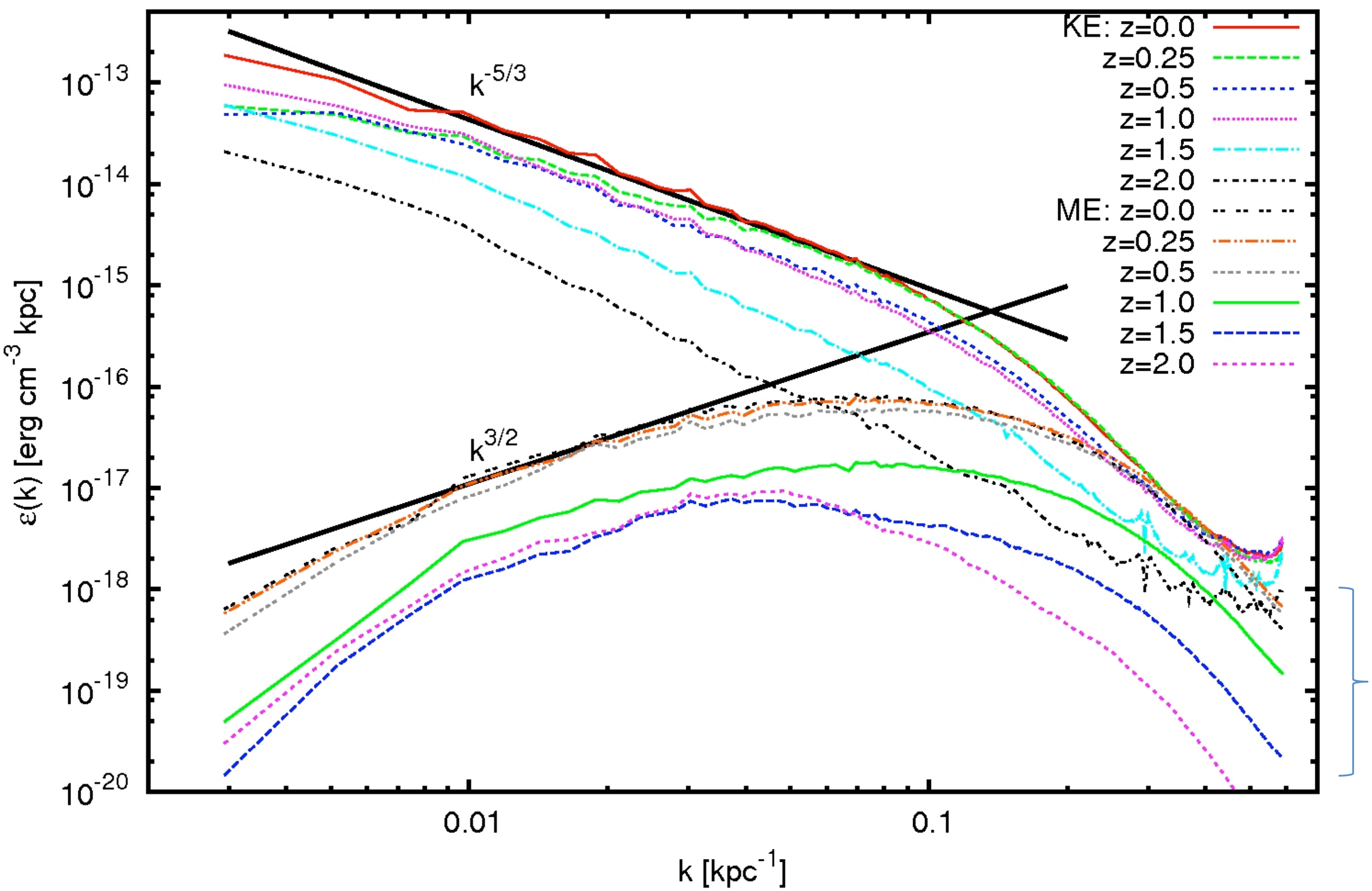

saturation

exponential growth

Diffusion of B

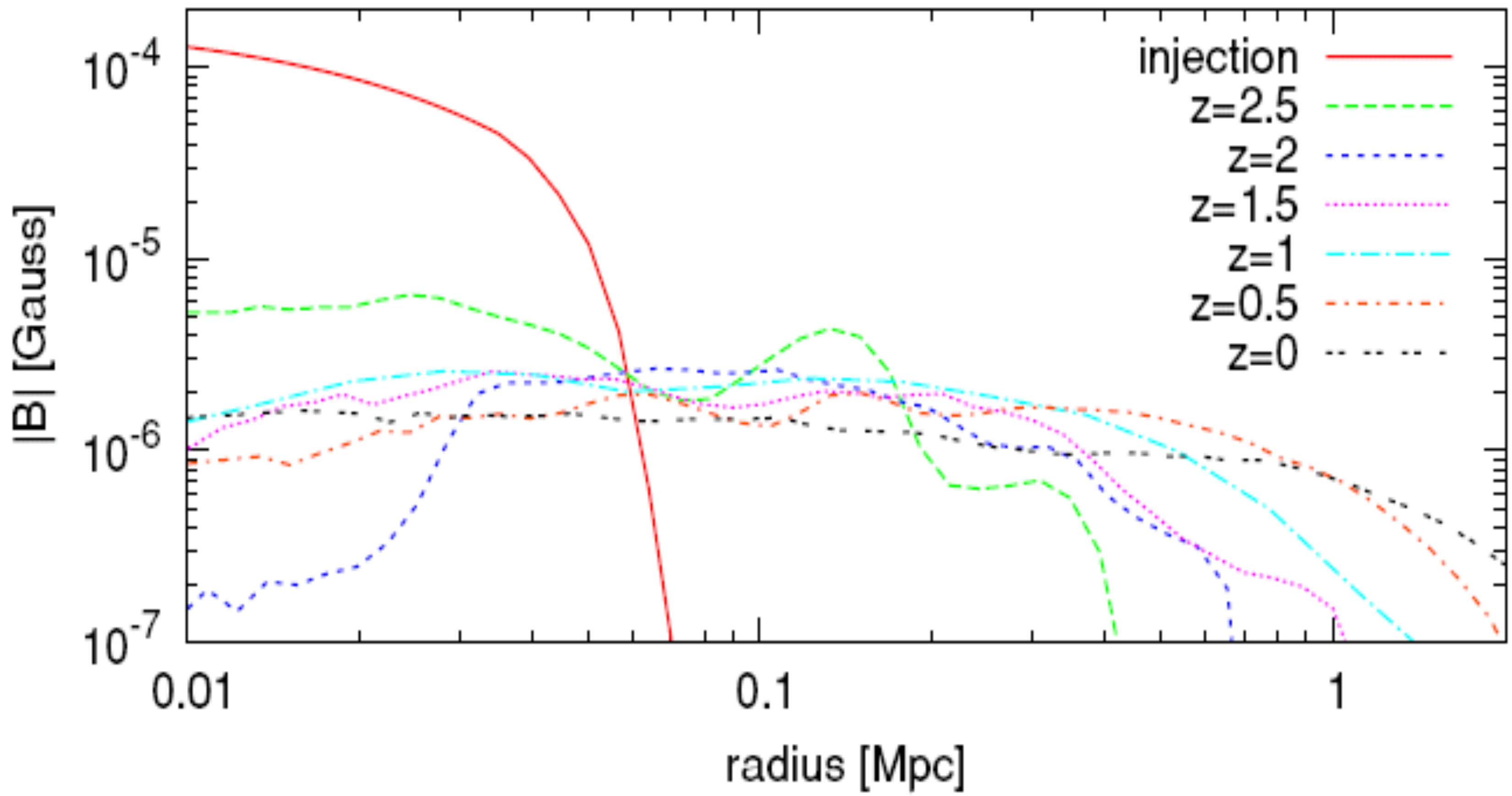

Synthetic FRM Map

- +/- 500 rad/m^2 max
- highest in cluster core, as observed
- banding due to field reversals, as observed
- filamentary structure on 40 kpc scale ($4\Delta x$)

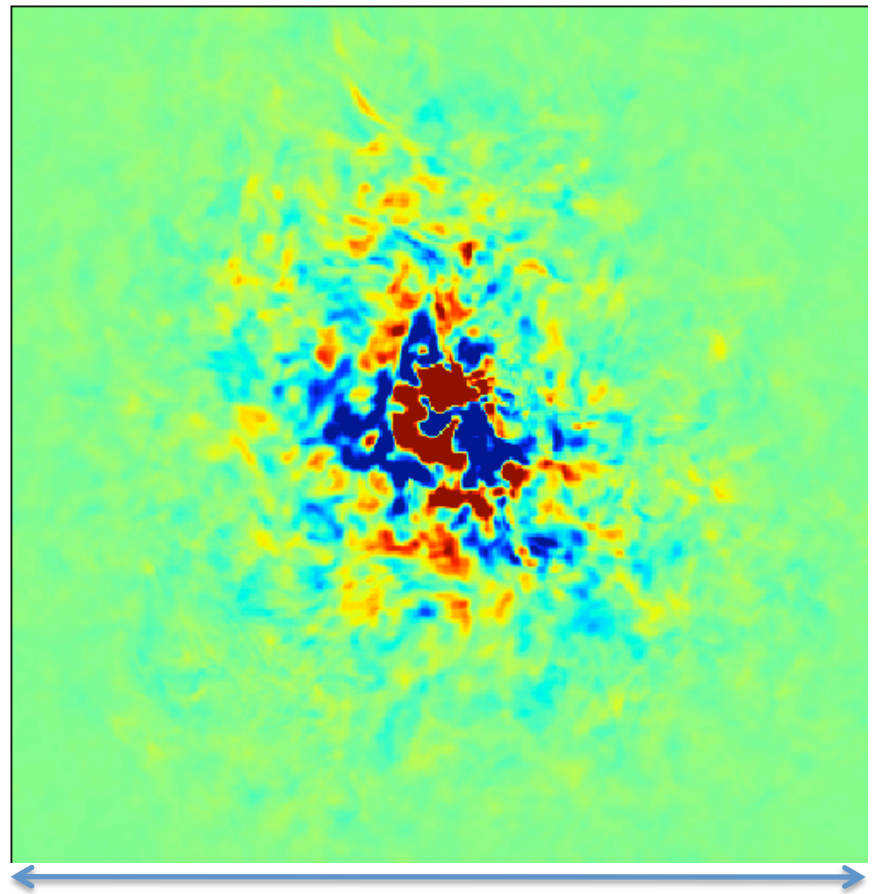

3 Mpc

Dependence on injection energy

- Varying magnetic energy injected over ~ 3 orders of magnitude at z=3 results in less than 1 order of magnitude magnetic energy at z=0
- B-fields still cluster filling

Xu et al. (2010)

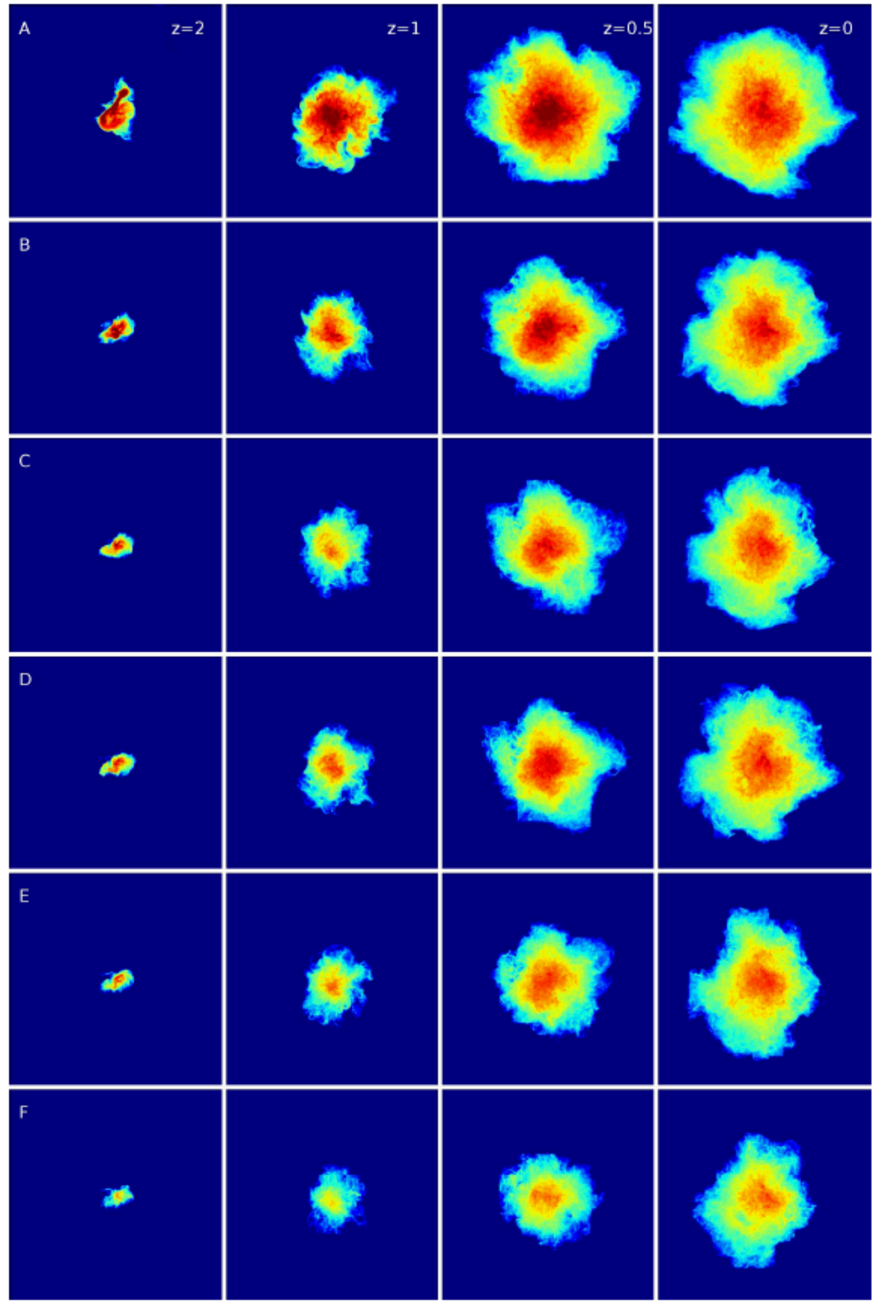

Evolution of magnetic energy

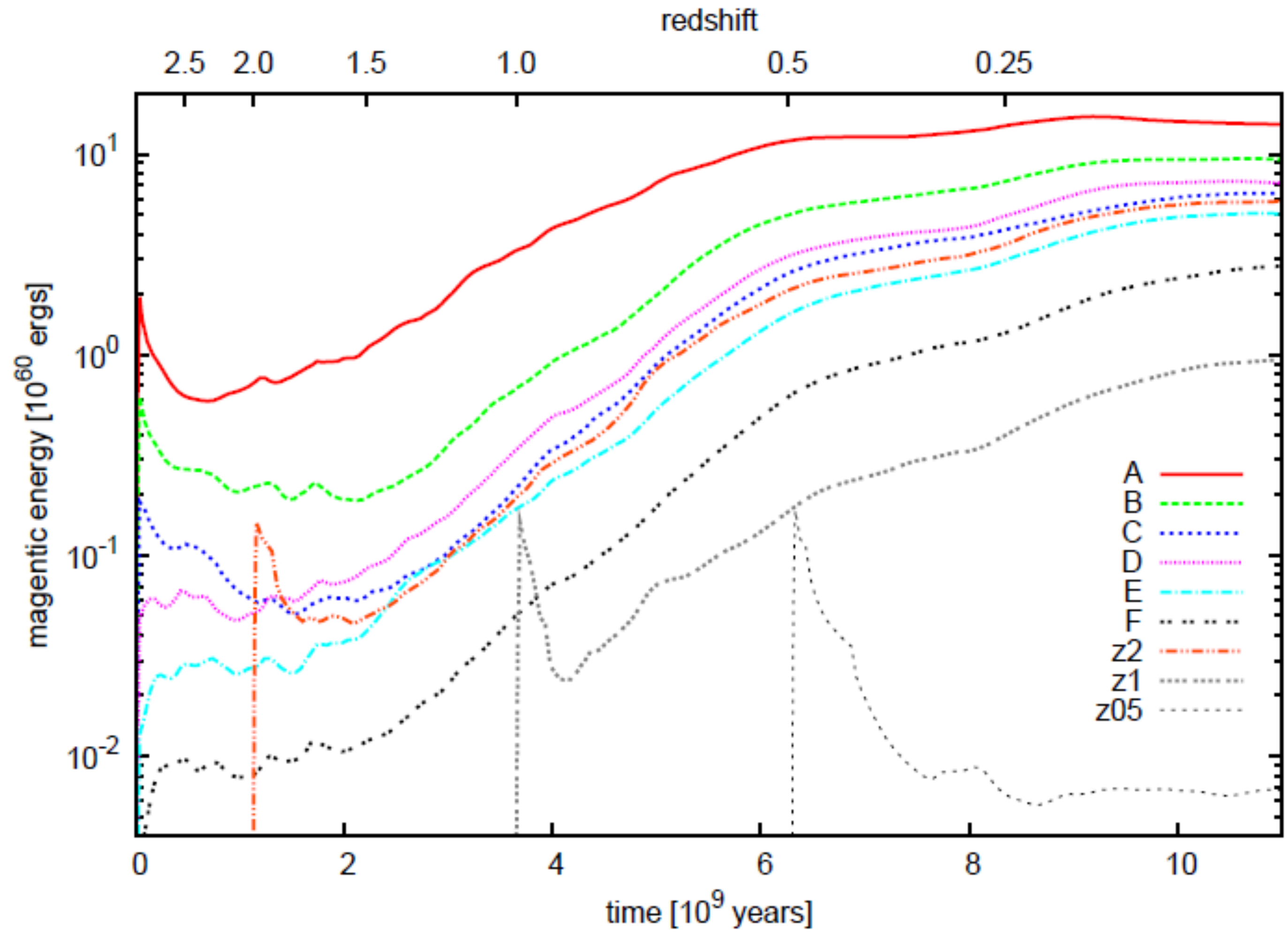

Xu et al. (2010)

Radial distribution of $|B_{rms}|$

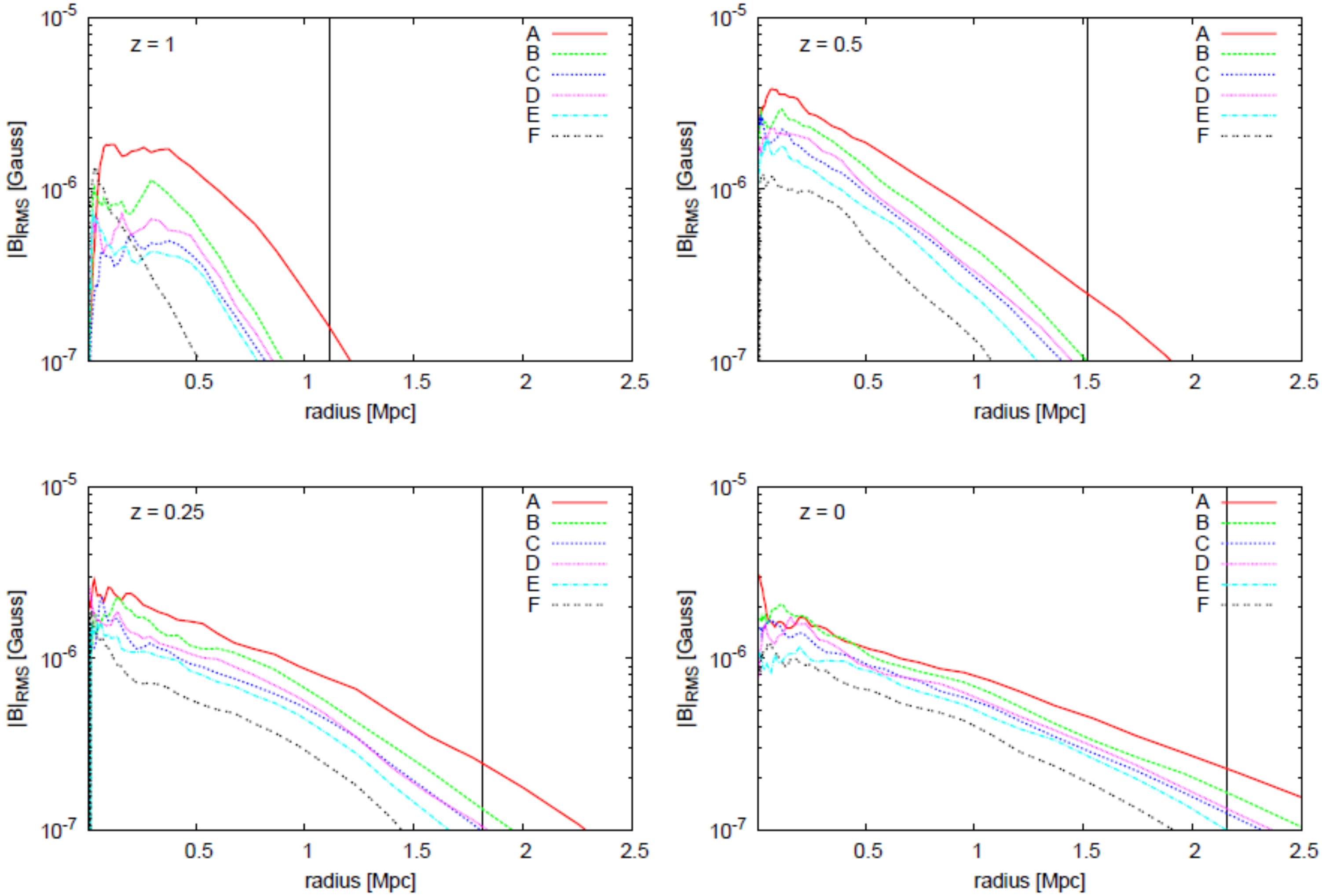

Xu et al. (2010)

Dependence on injection redshift

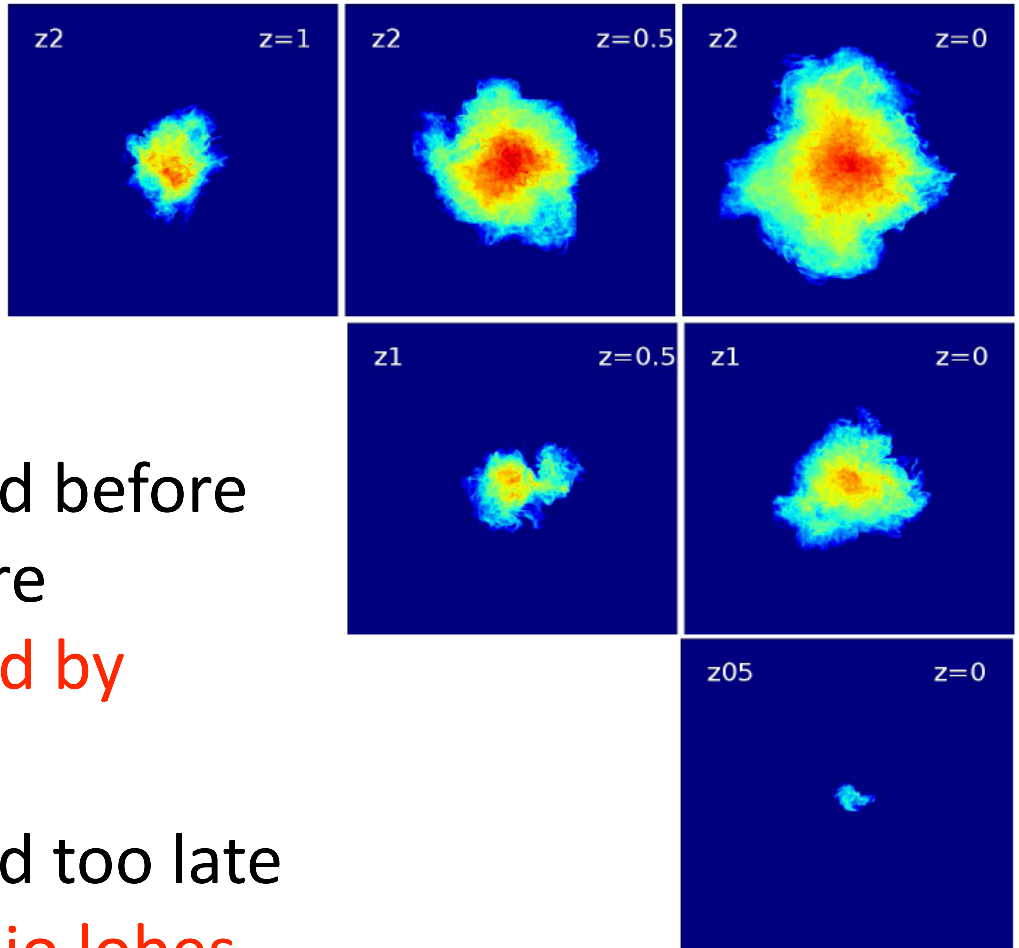

- Magnetic fields injected before cluster mass buildup are dispersed and amplified by cluster turbulence
- Magnetic fields injected too late remain confined to radio lobes

Xu et al. (2010)

Evolution of magnetic energy

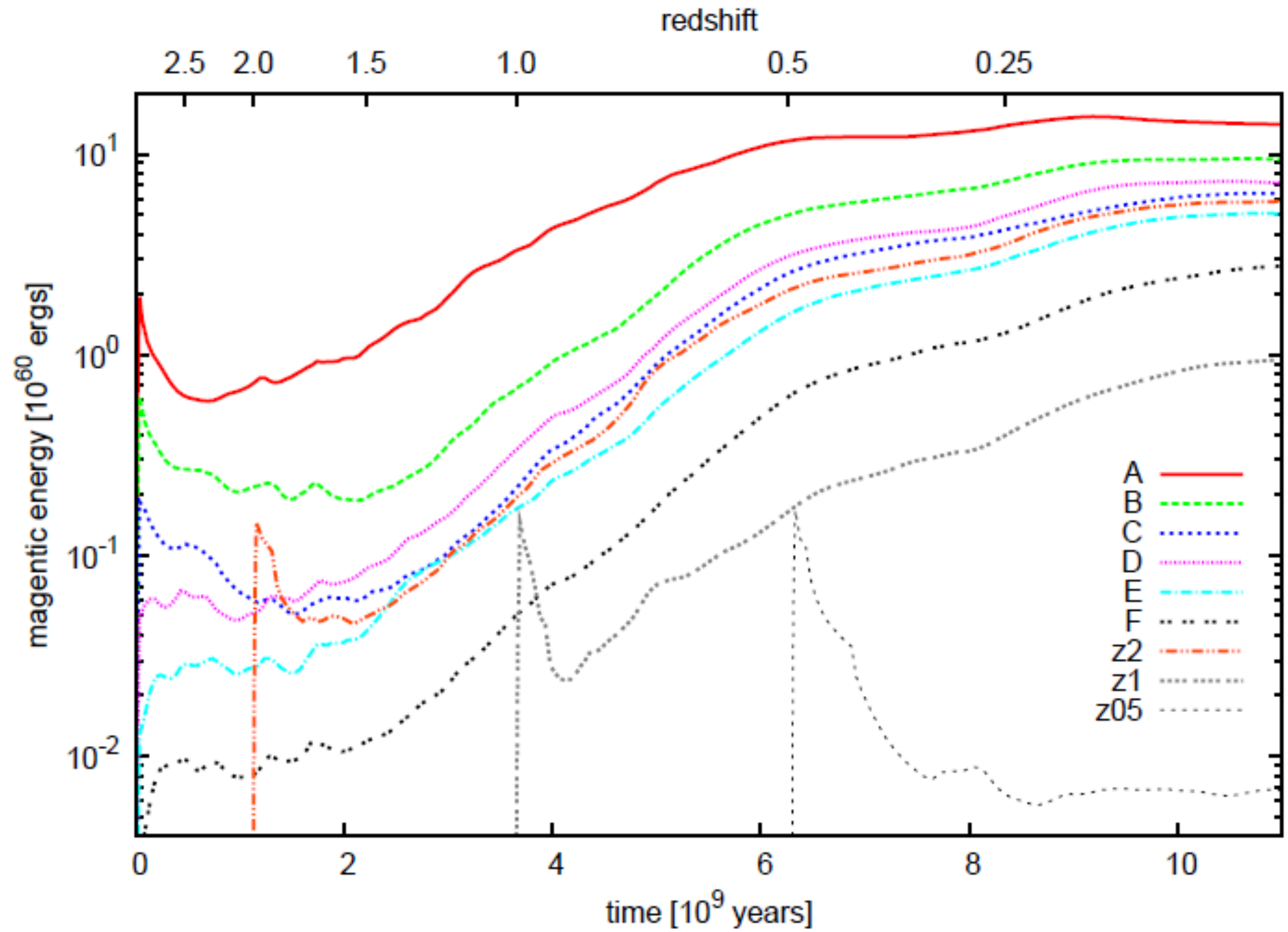

Radial distribution of $|B_{rms}|$

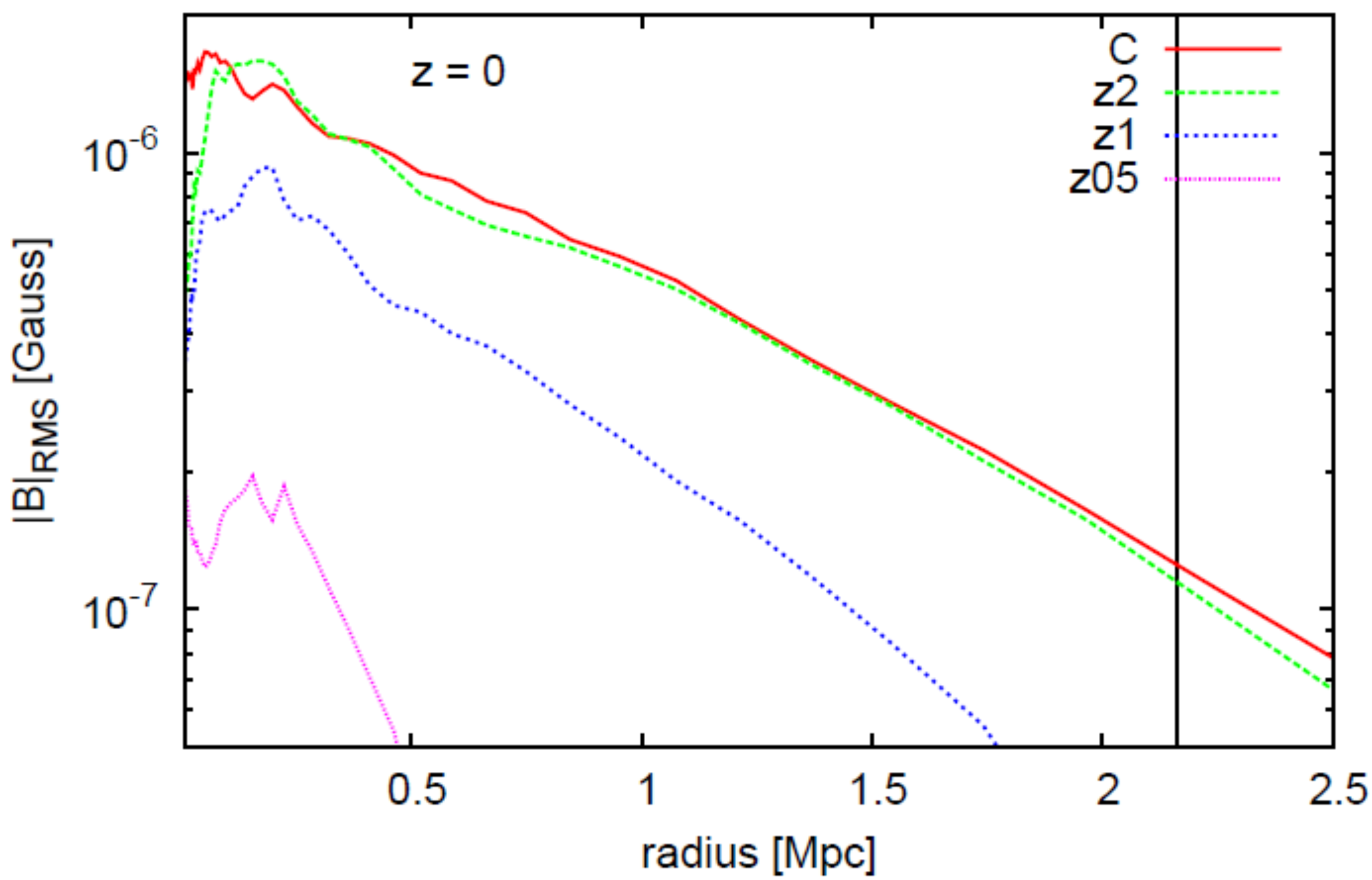

Conclusions

- A single powerful radio jet at high z can magnetize entire ICM to levels observed
  - Weakly sensitive on injected energy
- Timing of AGN injection important:
  - Early: cluster-wide B
  - Late: isolated bubbles
- Turbulent amplification and diffusion are the fundamental processes